# NUMERICAL ANALYSIS OF MIXED CONVECTION IN PULSATING FLOW FOR A HORIZONTAL CHANNEL WITH A CAVITY HEATED FROM BELOW

by

***Fatih SELIMEFENDIGIL***

Mechanical Engineering Department, Celal Bayar University, Manisa, Turkey

Original scientific paper
DOI: 10.2298/TSCI120413137S

*In this study, a channel with a cavity heated from below is numerically investigated for the mixed convection case in pulsating flow for a range of Richardson numbers (Ri = 0.1, 1, 10, 100) at Reynolds number of 50 in the laminar flow regime. At the inlet of the channel, pulsating velocity is imposed for Strouhal numbers between 0.1 to 1 and velocity amplitude ratio between 0.3 to 0.9. The effect of the pulsation frequency, amplitude, and Richardson number on the heat transfer enhancement is numerically analyzed. The results are presented in terms of streamlines, isotherm plots, and averaged Nusselt number plots. The fast Fourier transform plots for the Nusselt number response to single sinusoidal velocity forcing at the inlet and non-linearity in the response is also provided..*

Key words: *mixed convection, pulsating flow, computational fluid dynamics*

## Introduction

Mixed convection heat transfer is important for various engineering applications. Design of the heat exchangers, nuclear reactors, solar collectors, cooling of electronic equipments, and food industry may be considered as some of them where one has to improve the performance of those systems. Heat transfer and flow field characteristics have been investigated for the mixed convection case by many researchers [1-5].

When pulsations are applied to the flow system, heat transfer may be enhanced due to the change of the thickness of the boundary layer and thus the thermal resistance [6]. But, in the literature there exist also cases where pulsating flow does not effect [7] or even deteriorate heat transfer enhancement [8]. That means flow parameters and geometry of the problem may also have an effect on the heat transfer enhancement along with the pulsation [9-12]. A vast amount of literature is dedicated to examine the effects of pulsating flow on the heat transfer enhancement and self sustained oscillating flow. Kim *et al*. [13] have studied the pulsating flow and thermal transport from two heated blocks with different heights in a channel. The effects of various parameters, Strouhal number, height of the block on the heat transfer and fluid flow are analyzed. Greiner [14] have made experiments on hydrodynamic resonance and its effect on heat transfer in laminar flow. He observed that oscillatory perturbation at the frequency of the most unstable linear modes results in a resonance and significant heat transfer enhancement. Moon *et*

Authors' e-mail: fatih.selimefendigil@bayar.edu.tr

*al.* [15] have experimentally studied the effect of pulsating flow on the convective heat transfer from periodically spaced blocks in a channel. The experiment has been carried out for several parameters: frequency and amplitude of the pulsation and spacing between the blocks. They have showed that thermal transport from the blocks is affected by the parameter set. Pulsating flow at a backward facing step with a stationary cylinder is studied in [16]. Khanafer *et al*. [17] have numerically analyzed the mixed convection over a backward-facing step for laminar pulsating flow. Their results show that the average Nusselt number increases with an increase in Reynolds and Grashof numbers and decrease with the increase in the pulsating frequency. Boutina and Bessaih [18] have numerically studied the laminar mixed convection in an inclined channel containing two heat sources. The effects of the Reynolds number, spacing between the heat sources and the inclination angle on the heat transfer and flow field have been analyzed.

In the present work, mixed convection heat transfer in pulsating flow has been numerically investigated for a *T* shape channel with a cavity heated from below for a range of Richardson numbers, pulsating amplitude, and frequencies. The effect of the various parameters on the heat transfer enhancement is numerically analyzed. The results are presented in terms of streamlines, isotherms, and averaged Nusselt number for different parameters. The fast Fourier transform (FFT) plots for the Nusselt number response to different pulsating amplitudes and frequencies and non-linearity in the response are also provided.

## Numerical simulation

### *Problem description, governing equations, physical parameters, and solution method method.*

A schematic description of the problem is shown in fig. 1. A *T* shape channel is considered. The length and height of the channel are 21*L*, $H = L/2$, where *L* is the length of the square cavity. The whole channel walls are assumed to be adiabatic except the cavity which is kept at temperature $T_h$. The difference of temperature within cavity causes mixed convection that is produce entropy in cavity. At the inlet a sinusoidal velocity is imposed. Working fluid is air with Pr = 0.71. The flow is assumed to be 2-D, Newtonian, incompressible, and in the laminar regime. The physical properties are assumed to be temperature independent except for the density in the buoyant force according to Boussinesq approximation.

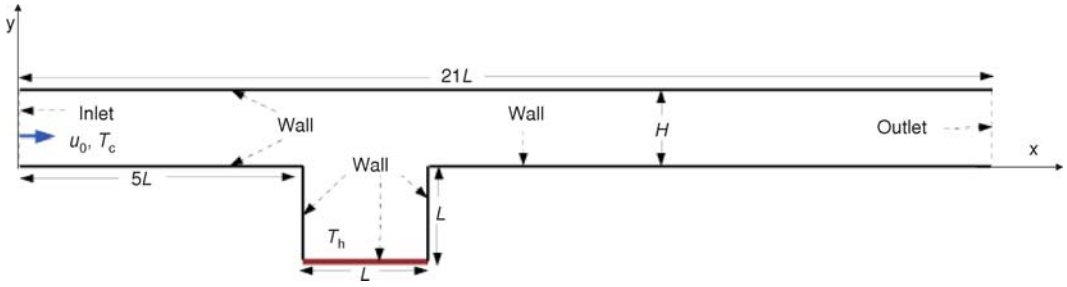


**Figure 1. Geometry and the boundary conditions for *T* shape channel. The cavity is heated from below (kept at temperature $T_h$ ). Air has a pulsating velocity $u_0 + Au_0 \sin(\omega t)$ and temperature $T_c$ at the inlet. All other walls except the bottom wall cavity are adiabatic**

By using the dimensionless parameters:

$$(U,V) = \frac{(u,v)}{u_0},\ (X,Y) = \frac{(x,y)}{H},\ \tau = \frac{u_0}{H}t,\ P = \frac{p}{\rho u_0^2},\ \theta = \frac{T - T_c}{T_h - T_c} \tag{1}$$

for a 2-D, incompressible, laminar, and unsteady case, the continuity, momentum, and energy equations can be expressed in the non-dimensional form:

$$\frac{\partial U}{\partial X}+\frac{\partial V}{\partial Y}=0 \tag{2}$$

$$\frac{\partial U}{\partial \tau}+U\frac{\partial U}{\partial X}+V\frac{\partial U}{\partial Y}=-\frac{\partial P}{\partial X}+\frac{1}{\mathrm{Re}}\left(\frac{\partial^2 U}{\partial X^2}+\frac{\partial^2 U}{\partial Y^2}\right) \tag{3}$$

$$\frac{\partial V}{\partial \tau}+U\frac{\partial V}{\partial X}+V\frac{\partial V}{\partial Y}=-\frac{\partial P}{\partial Y}+\frac{1}{\mathrm{Re}}\left(\frac{\partial^2 V}{\partial X^2}+\frac{\partial^2 V}{\partial Y^2}\right) \tag{4}$$

$$\frac{\partial \theta}{\partial \tau}+U\frac{\partial \theta}{\partial X}+V\frac{\partial \theta}{\partial Y}=\frac{1}{\mathrm{Pr}\,\mathrm{Re}}\left(\frac{\partial^2 \theta}{\partial X^2}\frac{\partial^2 \theta}{\partial Y^2}\right) \tag{5}$$

The relevant physical parameters are Reynolds number:

$$\mathrm{Re}=\frac{u_0 L}{v} \tag{6}$$

where $u_0$ denote the velocity imposed at the inlet and Richardson number:

$$\mathrm{Ri}=\frac{\mathrm{Gr}}{\mathrm{Re}^2} \tag{7}$$

where Gr represents the Grashof number:

$$\mathrm{Gr}=\frac{g\beta(T_\mathrm{h}-T_\mathrm{c})L^3}{v^2} \tag{8}$$

and Strouhal number is defined:

$$\mathrm{St}=\frac{fL}{u_0} \tag{9}$$

The boundary conditions for the considered problem in dimensionless form can be expressed:

- at the channel inlet, velocity is unidirectional and sinusoidal, temperature and velocity are uniform, $U = 1 + A\sin(2\pi\mathrm{St}\tau)$, $V = 0$, $\theta = 0$,
- on the bottom wall of the cavity, temperature is constant, $\theta = 1$,
- at the channel exit, gradients of all variables in the x-direction are set to zero, $\partial U/\partial X = 0$, $\partial V/\partial X = 0$, $\partial\theta/\partial X = 0$, and
- on the channel walls (except the bottom wall of the square cavity) adiabatic wall with no-slip boundary conditions are assumed, $U = 0$, $V = 0$, $\partial\theta/\partial n = 0$, where $n$ denotes the surface normal direction.

Local Nusselt number is defined:

$$\mathrm{Nu}_{\mathrm{x,t}}=\frac{h_{\mathrm{x,t}}L}{k}=-\left(\frac{\partial\theta}{\partial n}\right)_\mathrm{S} \tag{10}$$

where $h_{\mathrm{x,t}}$ represents the local heat transfer coefficient and $k$ denotes the thermal conductivity of air. The $\theta$ is the non-dimensional temperature which is defined as $\theta = (T - T_\mathrm{c})/(T_\mathrm{h} - T_\mathrm{c})$. The $n$ and $S$ denote the surface normal component (y-axis) and heated part of the surface (bottom wall of the cavity), respectively.

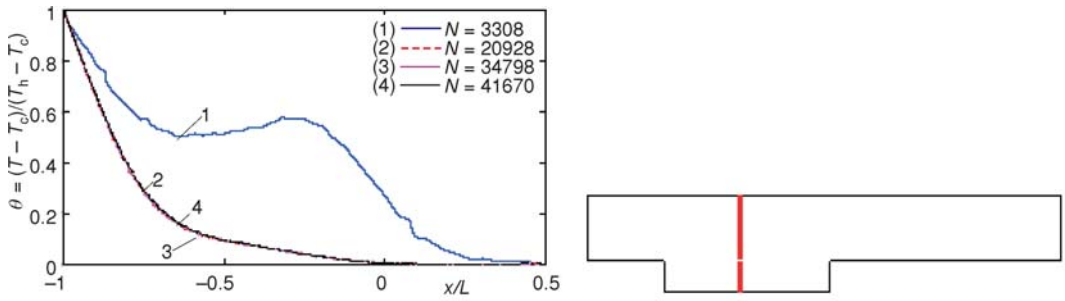


**Figure 2. Non-dimensionalized temperature staring from the middle of the bottom wall cavity ending at the upper wall of the channel along the vertical axis (vertical line on the right) for dierent grid sizes at Ri = 10**

Spatial averaged Nusselt number is obtained after integrating the local Nusselt number along the bottom wall of the cavity:

$$\mathrm{Nu}_{\mathrm{t}} = \frac{1}{L}\int_0^L \mathrm{Nu}_{\mathrm{x,t}}\,\mathrm{d}x \tag{11}$$

and both time and spatial averaged Nusselt number is obtained for one period of oscillation:

$$\mathrm{Nu} = \frac{1}{T}\int_0^T \mathrm{Nu}_{\mathrm{t}}\,\mathrm{d}t \tag{12}$$

Equations (2)-(5) along with the boundary and initial conditions are solved with FLUENT 6.1 solver (a general purpose finite volume solver). Second order upwind schemes are applied in terms of discretising the momentum and the energy equations. The PISO algorithm is used for pressure velocity coupling. The pressure-based segregated algorithm was used in FLUENT software. The system of algebraic equations is solved with Gauss-Siedel point by point iterative method and algebraic multi-grid method. The convergence criteria for continuity, momentum, and energy equations are set to $10^{-4}$, $10^{-5}$, and $10^{-5}$, respectively. The body-adapted mesh consists of 20928 triangular elements and is refined close to the cavity. Mesh independence of the solutions has been confirmed. Non-dimensionalized temperature starting from the middle of the bottom wall cavity ending at the upper wall of the channel along the vertical axis is shown in fig. 2 for different grid sizes $N$ at Ri = 10. It is seen that the solution for 20928 elements is closer to the solution for 41670 elements. Time step size independence study is also carried out. Figure 3 shows the space-averaged Nusselt number at Ri = 100, St = 1, and $A$ = 0.6 for different time steps sizes. Time step size d$t$ = $\tau$/100 is chosen both for its accuracy and computational time where $\tau$ denotes the period of the oscillation. Steady solutions are used as the initial conditions for unsteady computations.

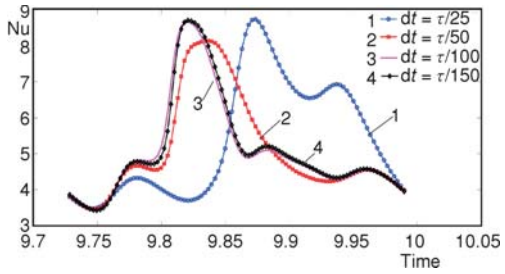


**Figure 3. Space-averaged Nusselt number plots for dierent time step sizes**

## Results and discussions

In the present study, Richardson number is varied between 0.1 and 100 (Ri = 0.1, 1, 10, 100) and Reynolds number is kept at 50 in the laminar regime range. Calculated spatial aver-

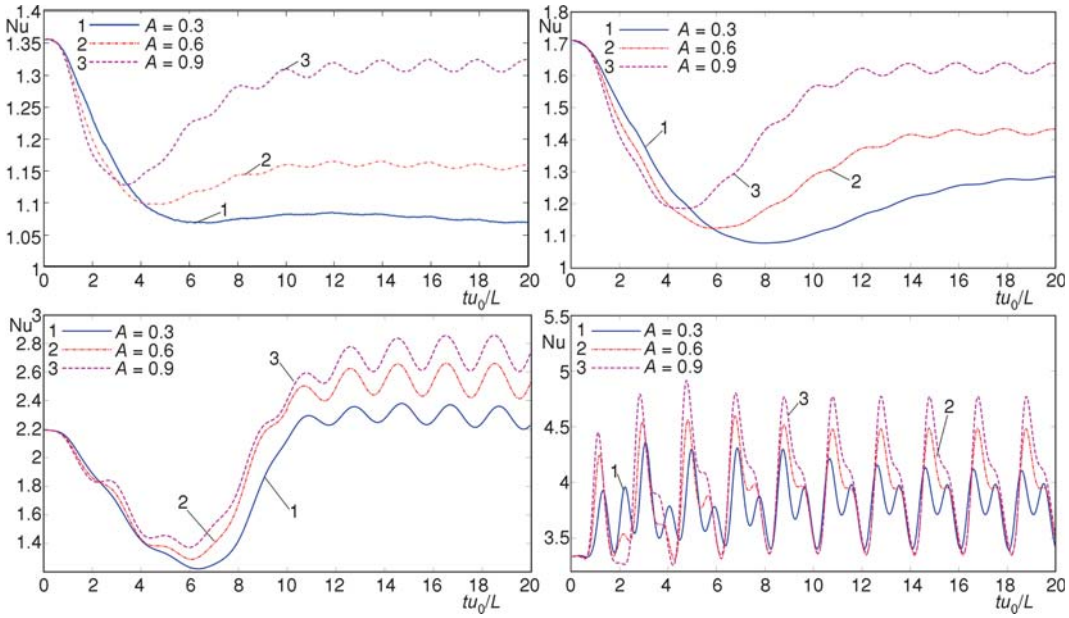


**Figure 4. Spatial averaged Nusselt number plots for Ri = 0.1, 1, 10, and 100 (from top to bottom) at St = 0.1 for dierent velocity amplitudes**

aged Nusselt number plots are shown for St = 0.1 in fig. 4 and for St = 1 in fig. 5 at Richardson numbers of 0.1, 1, 10, and 100, respectively. Non-linearity which is seen as the distortion from

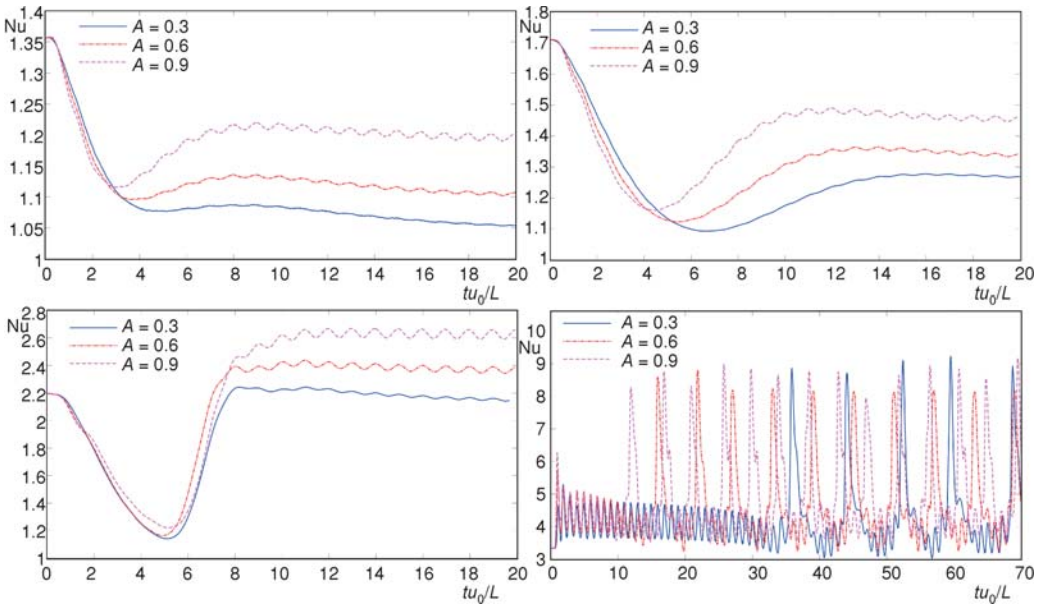


**Figure 5. Spatial averaged Nusselt number plots for Ri = 0.1, 1, 10, 100 (from top to bottom) at St = 1 for dierent velocity amplitudes**

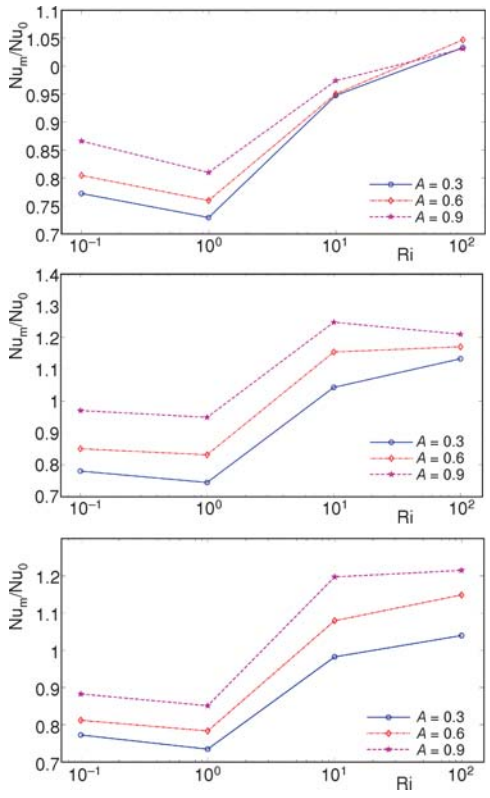


**Figure 6. Time and spatial averaged Nusselt number *vs.* Richardson number for dierent velocity amplitudes at St = 0.1, 0.5, 1 (from top 7 to bottom)**

the pure sinusoid for Ri = 100 for both St = 0.1, and St = 1. At Richardson numbers of 0.1,1 and 10, after a transient region, the system reaches its periodic state with one dominant frequency which is the forcing frequency. At Ri = 100 and St = 1, after the initial transients, the system reaches periodic state with the dominant frequency which is not the fundamental forcing frequency.

Time averaged values of the Nusselt numbers for pulsating flow divided by non-pulsating case (heat transfer enhancement) are shown in fig. 6 for St = 0.1, 0.5, 1, respectively. Heat transfer is generally increasing with increasing the Richardson number. Heat transfer enhancement also increases with an increase in the velocity amplitude. At St = 0.1, maximum heat transfer enhancement is less than 5% which is achieved at Ri = 100 and at velocity amplitude of 0.9. At St = 0.1 and Ri = 100, heat transfer enhancement achieved at velocity amplitude of 0.6 is higher than the value achieved at velocity amplitude of 0.9. At St = 0.5, heat transfer increases at about 25% for Ri = 10 and velocity amplitude of 0.9. At St = 1, 20% of heat transfer enhancement is achieved at Ri =100 and velocity amplitude of 0.9.

Streamline and isotherm plots for Ri = 100 at velocity amplitudes 0.3 (heat transfer enhancement 1%) and 0.9 (heat transfer enhancement 21%) are shown in fig. 8. The time instances within a period for two velocity amplitudes are shown in fig. 7. As it can be seen in the figure, the obtained regime is not really well oscillating, but it is illustrating a global behavior. As the Richardson number increases more flow is retained in the cavity. At the time when the Nusselt number is maximum, two main cells are seen and one of them is formed at the left side of the cavity. The isotherm plot at that time instance shows that maximum temperature gradient occurs in the middle of the bottom wall of the cavity and boundary layer becomes thicker towards the left and right sides of the cavity bottom wall. Temperature contours spreads inward on the left hand side, and outward towards the main flow on the right side of the cavity. As the time increases, when the Nusselt number decreases, two cells coalesce and the formation of the secondary vortex is seen on the right side of the cavity bottom wall. Isotherm plots show that, the extent of the high temperature gradient decreases towards the right and left sides of the bottom wall of the cavity and the spreading of the isotherms in the channel is due to the forced convection rather than the buoyancy effect.

For velocity amplitude of 0.9, streamline plots and isotherms in fig. 9 show the similar trend as for velocity amplitude of 0.3. At the time instance when the Nusselt number is maximum, the cell appearing in the channel penetrates more into the cavity. For the time instance

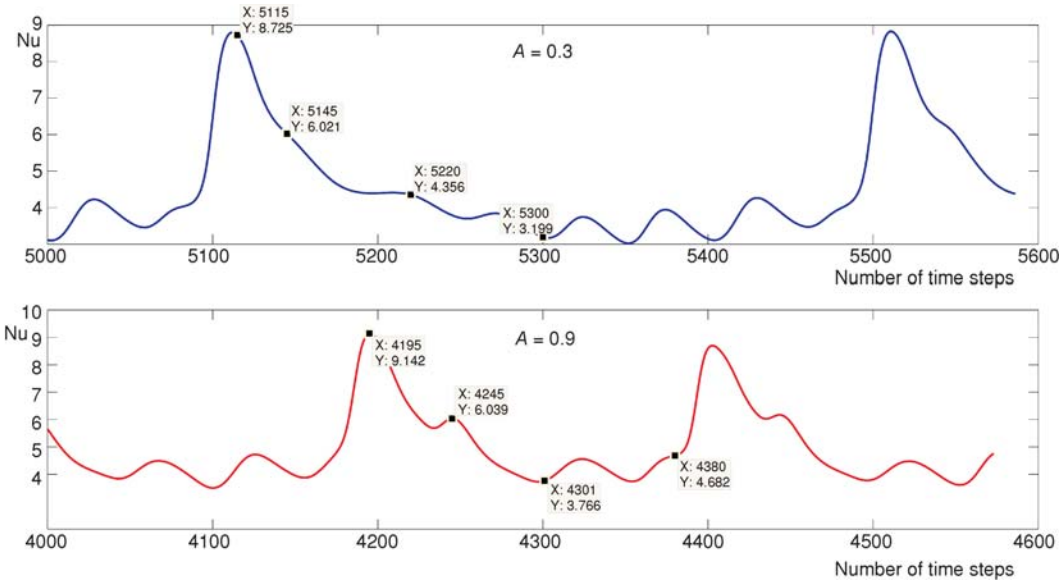


**Figure 7. Time instances with markers within a period at Ri = 100, St = 1 for velocity amplitude of 0.3 (top) and 0.9 (bottom)**

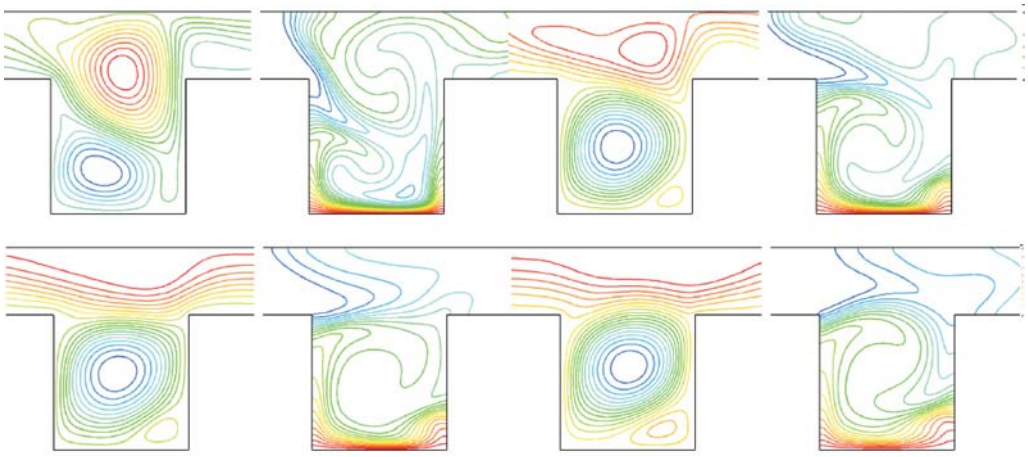

**Figure 8. Streamlines and isotherms taken for time instances according to fig. 7 (top) at Ri = 100, St = 1 and velocity amplitude ratio of 0.3**

when the Nusselt number is minimum, the strength and extent of the cell appearing on the right side of the cavity bottom wall is more compared to the case for velocity amplitude ratio of 0.3.

The FFT plots for (Ri = 10, St = 0.1) and (Ri = 100, St = 0.1) are shown in fig. 10. For Strouhal number of 0.1, at Ri = 10, with increasing amplitude, several peaks which are at the integer multiples of fundamental harmonic (forcing frequency) appear. At Ri = 10, for velocity amplitude of 0.9, these peaks which are the indications of the distortion from the linearity, disappear. The FFT plot at St = 1 for Ri = 100 shows several peaks which are at non-integer mul-

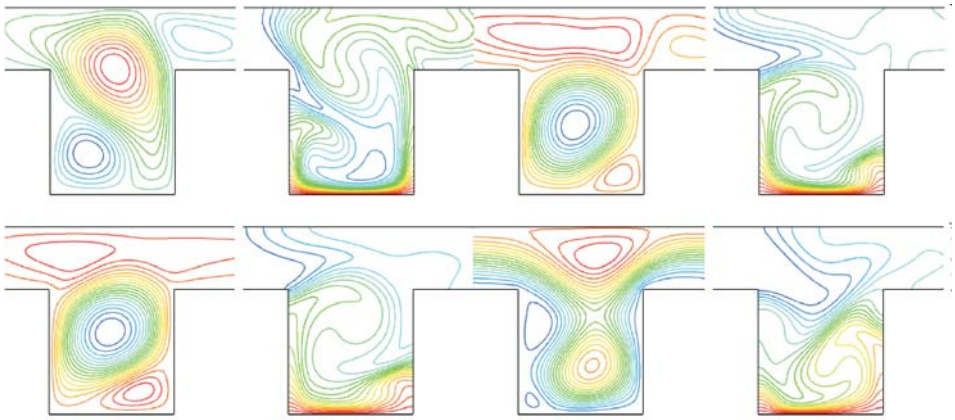

**Figure 9. Streamlines and isotherms taken for time instances according to fig. 7 (bottom) at Ri = 100, St = 1 and velocity amplitude ratio of 0.9**

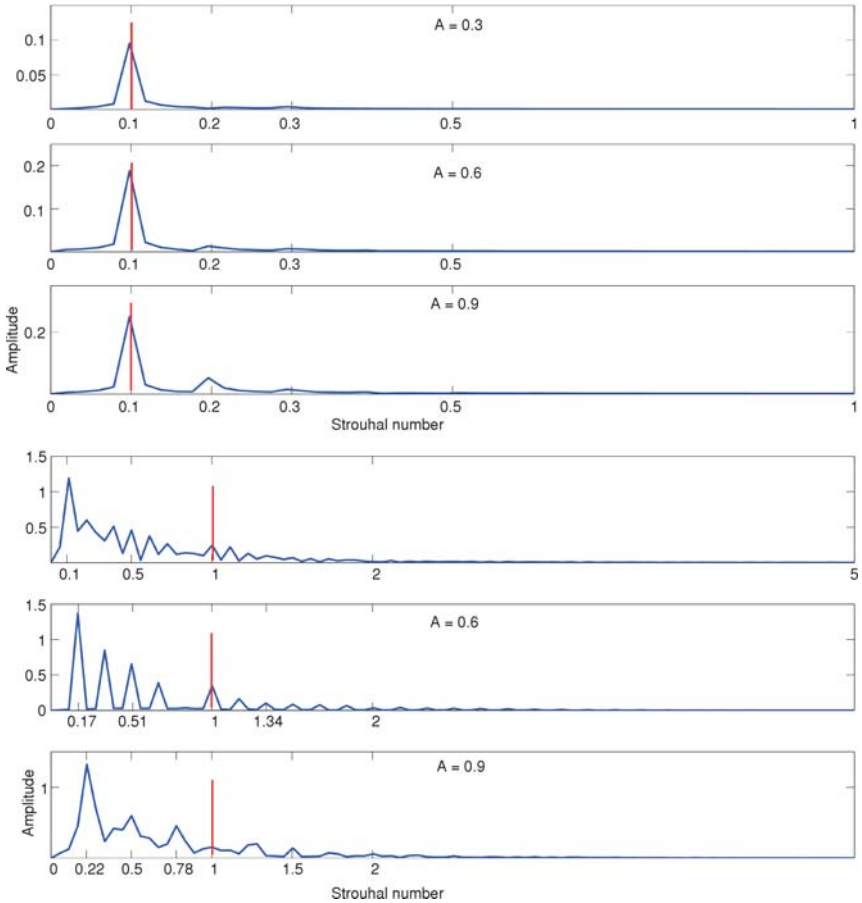


**Figure 10. FFT plots for Ri = 10 at St = 0.1 (first three plots), Ri = 100 at St = 1 (last three plots)**

tiples of the forcing frequency. These plots show the complicated interaction between the forced convection and natural convection. These plots are also important when one tries to get a mathematical model for the input (velocity forcing at the inlet) – output (Nusselt number at the bottom wall of the cavity) from the system identification [19].

## Conclusions

In this study, a channel with a cavity heated from below is numerically investigated for the mixed convection case in pulsating flow for a range of Richardson numbers (Ri = 0.1, 1, 10, 100) at Re = 50 in the laminar flow regime. At the inlet of the channel, pulsating velocity is imposed for Strouhal numbers between 0.1 to 1, and velocity amplitude ratio between 0.3 to 0.9. Following results are obtained.

- Generally heat transfer enhances with an increase in the velocity amplitude.
- Increasing the Richardson number generally enhances the heat transfer, but at Ri = 10 and at St = 0.5 and 1, more enhancement is obtained compared to the cases at Ri =100.
- Maximum heat transfer enhancement which is about 25% is obtained for the case at Ri = 10, velocity amplitude of 0.9, and St = 0.5
- For St = 0.1, at Ri = 10, with increasing amplitude, several peaks which are at the integer multiples of fundamental harmonic (forcing frequency) appear.
- For St = 1, at Ri = 10, the response is linear irrespective of the forcing amplitude.
- The FFT plot at St = 1 for Ri=100 shows a dominant peak which is at the 1/10 of the forcing frequency.

## Nomenclature

Gr – Grashof number (= $g\beta\Delta TL^3\nu^{-2}$), [–]
$g$ – gravitational acceleration, [ms$^{-2}$]
$H$ – height of the channel, [m]
$h$ – local heat transfer coefficient, [Wm$^{-2}$K$^{-1}$]
$k$ – thermal conductivity of the fluid, [Wm$^{-1}$K$^{-1}$]
$L$ – length of the cavity, [m]
$n$ – unit normal vector on the surface
$Nu_x$ – local Nusselt number, (= $hx/k$), [–]
$p$ – pressure, [Pa]
Pr – Prandtl number, (= $\nu/\alpha$), [–]
Re – Reynolds number, (= $u_0L/\nu$), [–]
Ri – Richardson number, (= Gr/Re$^2$), [–]
St – Strouhol number, (= $fL/\mu_o$), [–]
$T$ – temperature, [K]
$u, v$ – x-y velocity components, [ms$^{-1}$]
$x, y$ – Cartesian co-ordinates, [m]

### *Greek symbols*

$\alpha$ – thermal diffusivity, [m$^2$s$^{-1}$]
$\beta$ – fluid thermal expansion coefficient, [1/K]
$\theta$ – dimensionless temperature, (= $T - T_c/T_h - T_c$), [–]
$\nu$ – kinematic viscosity, [m$^2$s$^{-1}$]
$\rho$ – density of the fluid, [kgm$^{-3}$]

### *Subscripts*

c – cold
h – hot

## References

[1] Ozsunar, A., *et al*., Numerical Analysis of Grashof Number, Reynolds Number and Inclination Effects on Mixed Convection Heat Transfer in Rectangular Channels, *International Communications in Heat and Mass Transfer, 28* (2001), 7, pp. 985-994
[2] Aminossadati, S. M, Ghasemi, A., A Numerical Study of Mixed Convection in a Horizontal Channel with a Discrete Heat Source in an Open Cavity, *European Journal of Mechanics, 28* (2009), 4, pp. 590-598
[3] Dogan, A., *et al*., Investigation of Mixed Convection Heat Transfer in a Horizontal Channel with Discrete Heat Sources at the Top and at the Bottom, *International Journal of Heat and Mass Transfer, 49* (2006), 15-16, pp. 2652-2662
[4] Tmartnhad, I., *et al*., Numerical Investigation on Mixed Convection Flow in a Trapezoidal Cavity Heated from Below, *Energy Conversion and Management, 49* (2008), 11, pp. 3205-3210

[5] Selimefendigil, F., Oztop, H., Fuzzy-Based Estimation of Mixed Convection Heat Transfer in a Square Cavity in the Presence of an Adiabatic Inclined Fin, *International Communications in Heat and Mass Transfer, 39* (2012), 10, pp. 1639-1646
[6] Habib, M., *et al*., Heat Transfer Characteristics of Pulsated Turbulent Pipe Flow, *Heat Mass Transfer, 34* (1999), 5, pp. 413-421
[7] Mackley, M., Stonestreet, P., Heat Transfer and Associated Energy Dissipation for Oscillatory Flow in Baffled Tubes, *Chem. Sci. Eng., 50* (1995), 14, pp. 2211-2224
[8] Hemida, H., *et al.*, Theoretical Analysis of Heat Transfer in Laminar Pulsating Flow, *Int. J. Heat Mass Transfer, 45* (2002), 8, pp. 1767-1780
[9] Wang, Q., Jaluria,Y., Unsteady Mixed Convection in a Horizontal Channel with Protruding Heated Blocks and a Rectangular Vortex Promoter, *Phys. Fluids, 14* (2002), 7, 2113
[10] Fusegi, T., Numerical Study of Convective Heat Transfer from Periodic Open Cavities in a Channel with Oscillatory through Flow, *Int. J. Heat and Fluid Flow, 18* (1997), 4, pp. 376-383
[11] Selimefendigil, F., Numerical Analysis and POD Based Interpolation of Mixed Convection Heat Transfer Heat Transfer in Horizontal Channel with Cavity Heated from Below, *Engineering Applica- tions of Computational Fluid Mechanics, 7* (2013), 2, pp. 261-271
[12] Selimefendigil, F., Oztop, H., Numerical Analysis of Laminar Pulsating Flow at a Back- Ward Facing Step with an Upper Wall Mounted Adiabatic Thin Fin, *Computers and Fluids, 88* (2013), Dec., pp. 93-107
[13] Kim, S. Y., *et al*., Forced Convection Heat Transfer from Two Heated Blocks in Pulsating Channel Flow, *Int. J. Hear Mass Transfer, 41* (1998), 3, pp. 625-634
[14] Greiner, M. , An Experimental Investigation of Resonant Heat Transfer Enhancement in Grooved Channel, *Int. J. Heat Mass Transfer, 34* (1991), 6, pp. 1383-1391
[15] Moon, J. W., *et al*., Frequency-Dependent Heat Transfer Enhancement from Rectangular Heated Block Array in a Pulsating Channel Flow, *International Journal of Heat and Mass Transfer, 48* (2005), 23-24, pp. 4904-4913
[16] Selimefendigil, F., Oztop, H., Identification of Forced Convection in Pulsating Flow at a Backward Facing Step with a Stationary Cylinder Subjected to Nanofluid, *International Communications in Heat and Mass Transfer, 45* (2013), July, pp. 111-121
[17] Khanafer,K., *et al*., Mixed Convection Analysis of Laminar Pulsating Flow and Heat Transfer over a Backward-Facing Step, *International Journal of Heat and Mass Transfer, 51* (2008), 25-26, pp. 5785-5793
[18] Boutina, L., Bessaih, R., Numerical Simulation of Mixed Convection Air-Cooling of Electronic Components Mounted in an Inclined Channel, *Applied Thermal Engineering, 31* (2011), 11-12, pp. 2052-2062
[19] Selimefendigil, F., *et al.*, Nonlinear Identification of the Unsteady Heat Transfer of a Cylinder in Pulsating Cross Flow, *Computers and Fluids, 53* (2012), Jan., pp. 1-14

Paper submitted: April 13, 2012
Paper revised: September 4, 2013
Paper accepted: October 7, 2013